Modelling and simulation for energy management of a hybrid microgrid with droop controller

Khalil Saadaoui, Kaoutar Senhaji Rhazi, Youssef Mejdoub, Abderraouf Aboudou
Laboratory of Networks, Computer Science, Telecommunication, Multimedia (RITM), CED Engineering Sciences, Higher School of Technology, Hassan II University, Casablanca, Morocco

Article Info

Article history:

Received Jun 10, 2022
Revised Sep 3, 2022
Accepted Oct 1, 2022

Keywords:

Battery energy storage
Dynamic modeling
Hybrid AC-DC microgrids
Interlinking converter
MATLAB simulation
Primary droop control
Wind turbine

ABSTRACT

The most efficient and connected alternative for increasing the use of local renewable energy sources is a hybrid microgrid, these systems face additional challenges due to the integration of power electronics, energy storage technologies and traditional power plants. The hybrid alternating current-direct current (AC-DC) microgrid that is the subject of this research uses a primary-droop control system to regulate state variables and auxiliary services, thus, it is composed of batteries, solar panels and a miniature wind turbine (PDC) and controls how each energy source in a microgrid contributes to the final product. To achieve the given objectives, this paper will create appropriate models for each part of the microgrid design and define, among them, the energy storage batteries and power electronic converters required for each level of each of these systems. Finally, the dynamic nature of the system will be critically evaluated and characterized, to distribute the load and reduce imbalances, modify the primary drop of the resulting microgrid using MATLAB simulation.

Corresponding Author:

Khalil Saadaoui
Laboratory of Networks, Computer Science, Telecommunication, Multimedia (RITM), CED Engineering Sciences, Higher School of Technology, Hassan II University of Casablanca
Km 7 El Jadida Road-r.p.8, B.P. 20000, Casablanca, Morocco
Email: khalil.saadaoui@ensem.ac.ma

1. INTRODUCTION

Electricity may be kept accessible even when the weather changes or consumer demand increases by combining many energy sources [1]. In the event of unanticipated events or breakdowns, decentralized, updated versions of earlier, huge electric grids and microgrids face substantial challenges in preserving system resilience. Using a modular design, give operators considerable latitude. For instance, sophisticated direct current (DC) system improvements may be used with hybrid alternating current-direct current (AC-DC) microgrids [2]. DC microgrids are more suited than AC systems for integrating distributed energy resources (DER) [3], [4] and novel components due to their well-known dynamic models [5] and controlled protection requirements. Electricity may be produced in many places.

Adopting appropriate control strategies [6] and operational standards are additional difficulties for hybrid systems. The use of hierarchical control in hybrid, alternating current, and direct current microgrids has garnered a significant amount of interest [7], [8]. In the microgrid stage of global control, distributed generating units respond instantly to local variations of system variables brought on by shifts in demand or interruptions from the outside world [9]. This section also discusses how droop may be prevented or corrected. Due to the growing need for effective and flexible shared contributions from DER [10] in DC and AC sub-grids [11], research and modeling of predicted behavior under various operating conditions, as well as methods to evaluate control systems at various levels, have expanded dramatically [12], [13].

2. MODELING

The insulated-gate bipolar transistor (IGBT) power converter with filtering components supports the alternating current side of the microgrid because of its rapid dynamics [14] and internal control mechanism. A power flow, current controller, & filter make up the internal control system. Boost converters can handle a rise in demand or a fall in output. As a result, under these circumstances, a battery storage system may be employed as a backup Figure 1.

At the point-of-common-coupling (PCC), electricity generated by alternating current sources is exchanged with the electrical grid suitably using circuit breakers. A solar power plant that is comprised of solar panels and precisely managed MPPT boost converters is what makes up the direct current component of the system [15]. Batteries, solar power plants, and other AC-DC connection parts are connected via a second DC bus known as the main bus [16]. High capacitance DC bus components are required to smooth DC voltage. Loads of the DC microgrid are linked to the wider grid through a bus. Offshore wind turbines with voltage source converters (VSCs) installed [17], [18] may improve the reliability of the power system on oil and gas installations [19].

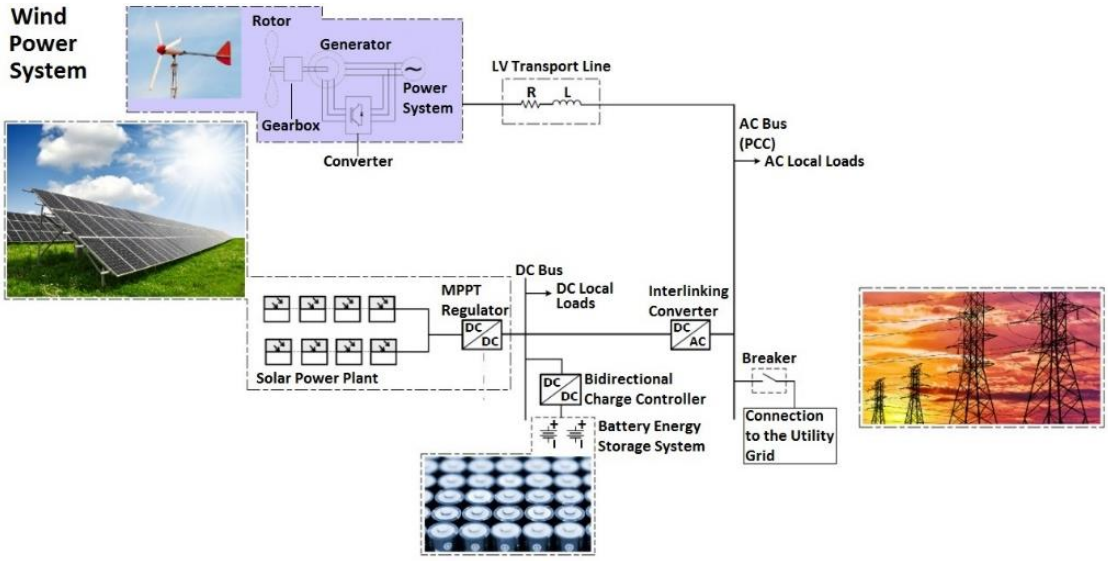

Figure 1. System overview

2.1. Modeling of wind turbine

The kinetic energy of the wind is converted into a useful form of mechanical energy by a device known as a wind turbine, the movement of the air molecules inside the mass as they move over the working surface of the turbine is what gives kinetic energy its material manifestation [17]. We can calculate the incident power of the wind (also known as the theoretical power) by using the Bernoulli theorem and the theory of momentum.

$$P_{\text{incident}} = \frac{1}{2}\rho . S . v^3 \tag{1}$$

where S is the surface swept by the blades of the turbine [m²], ρ is air density (ρ =1225 kg/m^3 at atmospheric pressure), and v is wind speed [m/s].

In a turbine, the rotor's power is extracted at a lower rate than the power impacting it.

$$P_{ext} = \frac{1}{2}\rho \cdot S . C_p(\lambda, \beta) \cdot v^3 \tag{2}$$

where Cp (λ, β) is the power coefficient, which describes the turbine's efficiency. It depends on the ratio λ. This ratio serves as a representation of the relationship between wind speed, orientation angle β, and turbine speed at the end of the blades.

$$\lambda = \frac{R \cdot \Omega_t}{v} \tag{3}$$

Following is how Albert Betz (1920) determined the maximum power coefficient Cp.

$$C_p^{max}(\lambda,\beta) = \frac{16}{27} \approx 0{,}593 \tag{4}$$

This coefficient depends on the constitution of the turbine. For a wind medium power, we have:

$$C_p(\lambda,\beta) = c_1 \cdot \left(c_2 \cdot \frac{1}{A} - c_3\beta - c_4\right) \cdot e^{-c_5}\frac{1}{A} + c_6 \cdot \lambda \tag{5}$$

Furthermore, as p is typically greatest for β = 0°, we can state that this turbine will operate at its most efficient level for a speed ratio λ [20], [21] of the order of 23. The coefficient of power is at its maximum value $CpMAX = Cp\ \lambda opt$ if the velocity ratio is kept at its ideal value λ*opt*. The wind turbine's [17] maximum power (6) and (7).

$$P_{opt} = \frac{1}{2}\rho \cdot S.C_{pMAX} \cdot v^3; \text{ with } v = \frac{R}{\lambda_{opt}}.\Omega_t \tag{6}$$

$$\text{So}, P_{opt} = \&\frac{1}{2}\rho.S.C_{pMAX} \cdot \left(\frac{R}{\lambda_{opt}} \cdot \Omega_t\right)^3 \tag{7}$$

We discovered that variations in *v*, wind speed, have a significant impact on wind power. Because the coefficient *Cp* is dependent on lambda and thus on *v* and from the relationship

$$Pext = \frac{1}{2}\rho.\ S.\ Cp(\lambda,\ \beta)\ .\ v\ 3$$

We see that power is inversely correlated with wind speed. Furthermore, it should be mentioned that the maximum power extracted changes with wind speed. The double fed induction generator (DFIG) can extract the most power at each time, making it a benefit to use a generator that adjusts to wind speed [22]. Ct is the torque at the turbine's slow axis:

$$C_t = \frac{P_{\text{ext}}}{\Omega_t} = \frac{1}{2}\rho \cdot S \cdot C_p(\lambda,\beta) \cdot v^3 \cdot \frac{1}{\Omega_t} \tag{8}$$

The total inertia *j* is the inertia of the turbine. It reduced the fast axis and the inertia of the generator *jg*.

$$j = \frac{j_t}{G^2} + j_g \tag{9}$$

The fundamental equation of dynamics can be written as (10).

$$j\frac{d\Omega_{Mec}}{dt} = C_M = C_t - C_{em} - f\Omega_{Mec} \tag{10}$$

2.2. Solar power plant model simplified

With a well-designed photovoltaic solar-centric technique, the maximum power point tracking (MPPT) [10bis] controller or boost converter [23] may be regarded of as a continuous source of power that is visible from the DC bus. The standard model and the quick dynamics of the boost converter are the basis for this assumption. The generator instantly supplies its output current

$$I_{PV} = \frac{P_{PV}}{V_{DC\,Bus}} \tag{11}$$

2.3. Modeling and control of the battery energy storage system (BESS)

The battery energy storage system (BESS) is made up of many battery cells that are connected to one another in the correct order in order to provide the required rated voltage, storage capacity, and current output. Charging and discharging are both operations that are carried out in the BESS using a bidirectional converter. Each battery cell in the system is correctly linked to the others so that the BESS can supply the appropriate voltage, storage capacity, and output current. This is done to guarantee that the BESS operates correctly. The charging and discharging processes that are carried out by the BESS are handled by a bidirectional converter.

Line current equations may be constructed using average switching locations and average switching times. This study uses a simplified model for Li-Ion batteries, and that model explains how the no-load voltage is dependent on the charge state, the polarization voltage during both charging and discharging, the polarization resistance, and the exponential factor [14]. At the time of release:

$$V_{OC} = E_0 - \underbrace{K\frac{Q}{Q-it}}_{\text{Polarization voltage}} \cdot it + \underbrace{A\exp(-B \cdot it)}_{\text{Exponential term}} - \underbrace{K\frac{Q}{Q-it}}_{\text{Polarization res.}} \cdot i^* \quad (12)$$

Polarization control changes the charging mode to reflect a quick rise in internal voltage and now offers:

$$R_p^{(Charge)} = K\frac{Q}{it - 0.1 \cdot Q} \quad (13)$$

Classic proportional integral (PI) control of voltage and current can be used. Not stated here is the driver design.

2.4. Interlinking converter

2.4.1. Dynamic model

The interlinking converter (IC), a crucial component of hybrid microgrids, allows energy to be moved from one alternating current source to another while also enhancing system stability. A three-phase converter with a built-in filter is seen in Figure 2 before being linked to an AC system [8].

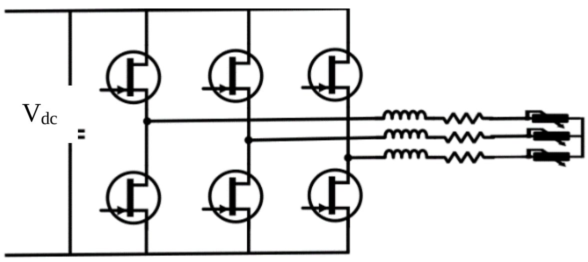

Figure 2. DC-microgrid/inverter/AC-microgrid association

The current line equations can be written in a rotating d-q frame with typical offset positions.

$$\frac{di_f^d}{dt} = -\frac{R_f}{L_f}i_f^d + \omega i_f^q + \frac{1}{L_f}\left(\frac{1}{2}V_{dc}d_d - v_{ac}^d\right) \quad (14)$$

$$\frac{di_f^q}{dt} = -\frac{R_f}{L_f}i_f^q - \omega i_f^d + \frac{1}{L_f}\left(\frac{1}{2}V_{dc}d_q - v_{ac}^q\right) \quad (15)$$

PCC voltage can be expressed as (16) and (17).

$$\frac{dv_{ac}^d}{dt} = \omega v_{ac}^q + \frac{1}{C_f}i_f^d - \frac{1}{C_f}i_{ac}^d \quad (16)$$

$$\frac{dv_{ac}^q}{dt} = -\omega v_{ac}^d + \frac{1}{C_f}i_f^q - \frac{1}{C_f}i_{ac}^q \quad (17)$$

The DC bus voltage is established by (18).

$$C\frac{dv_{dc}}{dt} = i_{dc} - \frac{3}{2}\left(i_f^d d_d + i_f^q d_q\right) \quad (18)$$

2.4.2. Control of the IC

Direct control of power flow in all directions, including active and reactive power, is one of the primary concerns of IC. It is necessary to have a PI controller as well as a decoupled d-q current. Figure 3 shows control diagram of the interlinking converter.

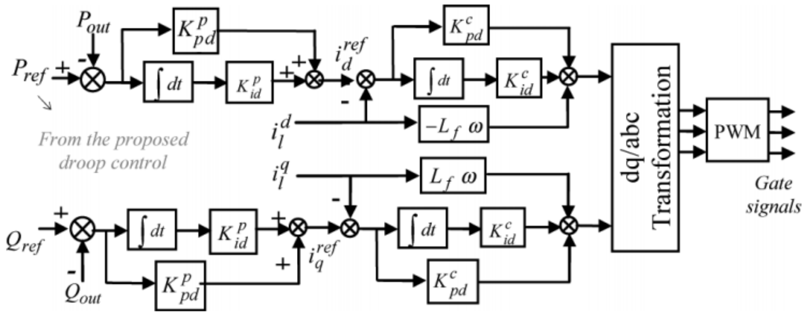

Figure 3. Control diagram of the interlinking converter

3. RESULTS AND DISCUSSION

According to the IEEE Standards Association [24], microgrids are small, autonomous grids that may function without connection to the larger grid. In active power management, the generators in a microgrid adapt their power output to the frequency fluctuation since the demand is always shifting. The following equations may be used to explain how active power output and frequency relate to one another.

$$DP = P2 - P1 = Sp(f1 - f2)$$

where *DP* represents the fluctuation in power output of the generator, *Sp* represents the reciprocal of the slope of the curve, and kW/Hz or MW/Hz is determined by the parameters of each DG. Voltage control: i) active power and frequency have a linear connection that is comparable to that of reactive power and terminal voltage' and ii) the reactive power output of micro sources may be changed to regulate the system voltage, an established method of managing an independent network is droop control. In reality, the functionality of a synchronous generator in a transmission system is imitated by damping controls for active power/frequency (P/F) and reactive power/voltage (Q/V), respectively. In delay avoidance mode, because all converters arrive at the same frequency, a phase-locked loop (PLL) is not necessary to complete system synchronization. Because all drives arrive at the same frequency, complete system synchronization is possible. Because each converter delivers electricity in proportion to its capacity, it may also share power.

3.1. Simulation

To construct the microgrid, a point-of-common-coupling (PCC) is used to link three identical inverter subsystems, each of which has an output of either 500, 300, or 200 kW Figure 4. The overall charge of the microgrid is determined by using the concept of dynamic charge. The micro-network monitoring system will if at all feasible, adjust the delay settings of the P/F and Q/V converters to ensure that the voltage and micro-frequency networks will eventually revert to their respective nominal levels (60 Hz and nominal values). Conventional renewable energy production systems include an inverter subsystem that consists of a two-position three-phase motor, an LC sludge motor, a 480/600 V motor, and the best DC power supply that will operate as the link (such as photovoltaic (PV) arrays, wind [25] turbines, energy storage systems for domestic batteries). A control system and a pulse width modulation (PWM) generator that powers the inverter are supplementary components of each subsystem. Controlling the drop control is one of the most important parts of the inverter control system. The drop control for the inverter is represented by the number. Because the inverter is not generating any active power and Slow P/F is set to 1, the frequency of the microgrid may vary from 60.3 to 59.7 Hz (the inverter is responsible for producing the active power that is rated for it). The converter supplies the whole of the inductive power, therefore the microgrid machine's PCC voltage may range from 612 Vrms down to 588 Vrms when the slow Q/V setting is adjusted to 4. The converter results in the generation of capacitive power in its entirety. Keep in mind that the reciprocal of Pnom's active force is equal to the maximum value of Qmax. Phnom is the abbreviation for the nominal active force. The dimensional subsystem of the station determines the station's reactive and active power consumption based on the frequency value that was supplied by the droop driver [25], [26]. In addition, a micro-network PCC machine is used to compute the d-q factors of the three-phase voltages and currents. Power dividers voltage regulators and drop control are both a part of the Reference Vref package. Once again, the controllers that use the measured voltages d-q in addition to the reference voltage Vref are the ones that activate the reference currents Id ref and Iq ref that are used by the current controllers. The reference currents, Id ref and Iq ref, are sent to the controllers of the current flow. The controllers will recycle the measured currents as well as the reference currents to give the driver with the necessary voltages d-q (VdVq Conv). It is important to keep in mind that dynamic controllers benefit from sophisticated computations [14]. Measurements are taken, and the PWM modulator Vref, which is also responsible for generating the inverter clock [20], [22], [23], converts the creation of Vref VdVq Conv to a three-phase signal.

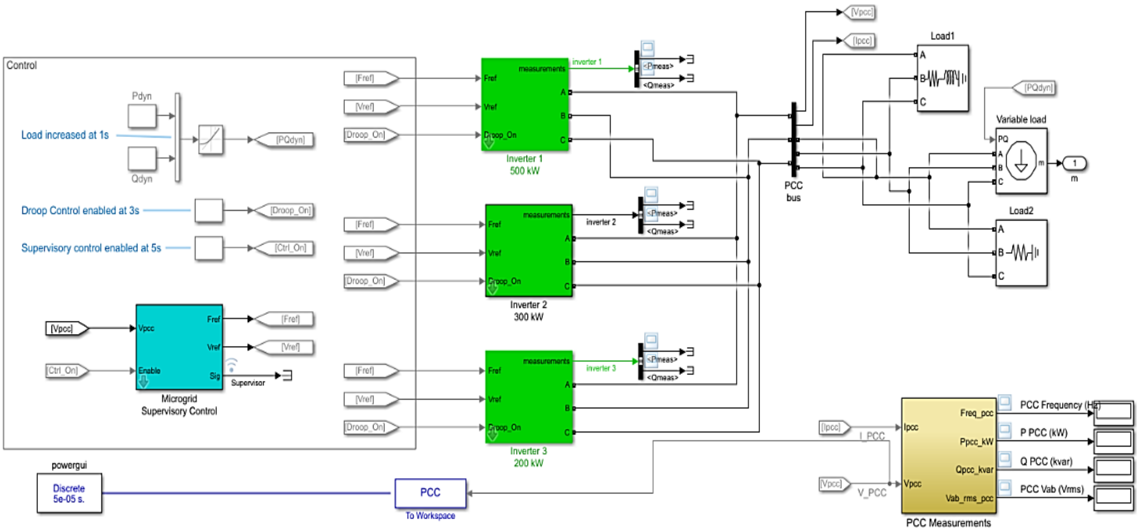

Figure 4. Hybrid AC-DC microgrid with primary droop control design using MATLAB/Simulink

3.2. Results analysis

To examine how well the controller is doing, the full model was built in MATLAB/Simulink Figure 4. The inverter is modeled in islanded mode and employs a P-f/Q-V droop control method. A DG arrangement with a single DG source driving three-phase loads is shown in Figure 2.

Due to the rise in reactive and active power, it is predicted that the operating frequency and voltage will be lower than no-load values. A 1% P/F step load is utilized to test the controller's response. The initial load connected to the network is a 450 KW/100 KVAR load. According to the findings shown in Figure 5, a drop in the inverter's output voltage is accompanied by an increase in the corresponding demand for reactive power and a reduction in the operating frequency, both of which are established by the frequency droop coefficient that has been provided.

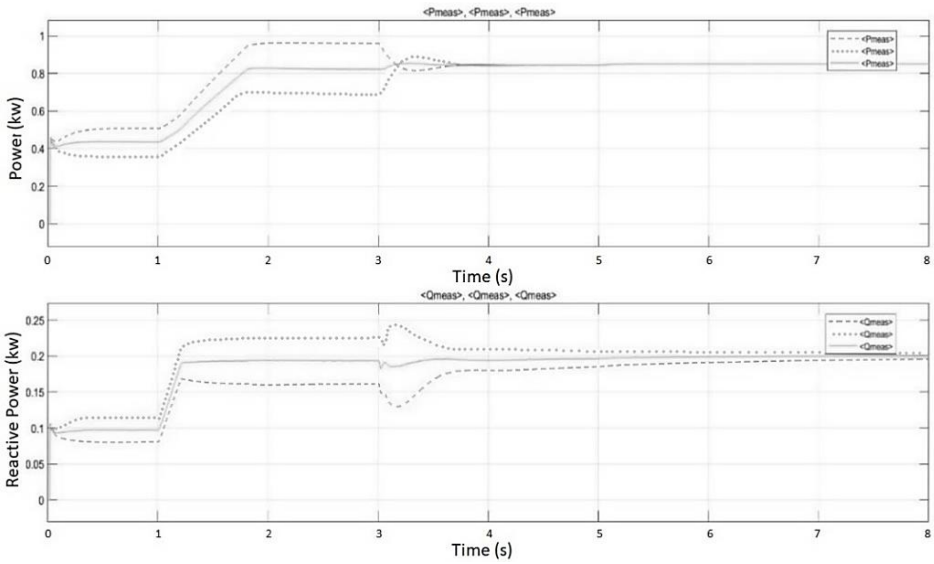

Figure 5. Simulation scope of power flow in the hybrid AC-DC microgrid with primary droop control

The frequency ranges from 59.7 Hz all the way up to 60.3 Hz, however the inverter does not produce any active electricity at the 60.3 Hz setting (inverter producing its rated active power). Figure 6 illustrates an increase in both active and reactive power (a). It shows how, at t=5 seconds, the controller reduces the operating voltage to accommodate the change in reactive load.

Because the droop Q/V is set to 4%, the voltage of the microgrid at the PCC bus is permitted to fluctuate between 612 and 588 Vrms (the inverter supplying all of its inductive power). The formula for determining Qmax is Phnom divided by fifty percent of the rated active power. The process of dynamically adjusting the total dynamic load of the microgrid is shown in Figure 7, which shows how the dynamic load model is employed. At the circuit junction in issue, the connection between the smaller grid (the microgrid) and the bigger grid (the larger grid) is created. The PLL is not necessary to maintain system-wide synchronization since, when utilizing the droop controller technique, all inverters achieve the same frequency.

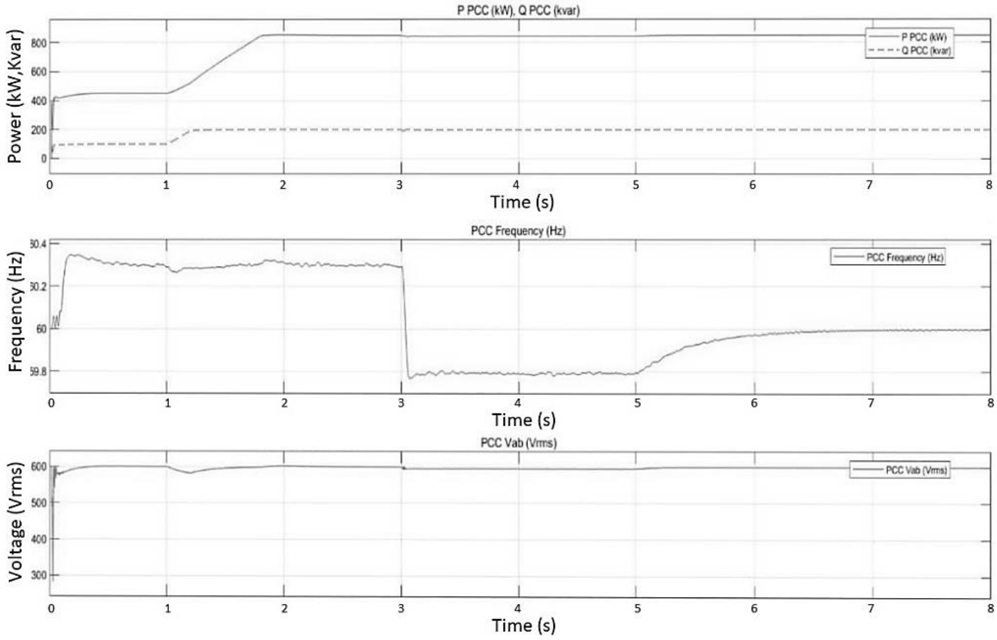

Figure 6. Active power and frequency in the hybrid AC-DC microgrid with primary droop control

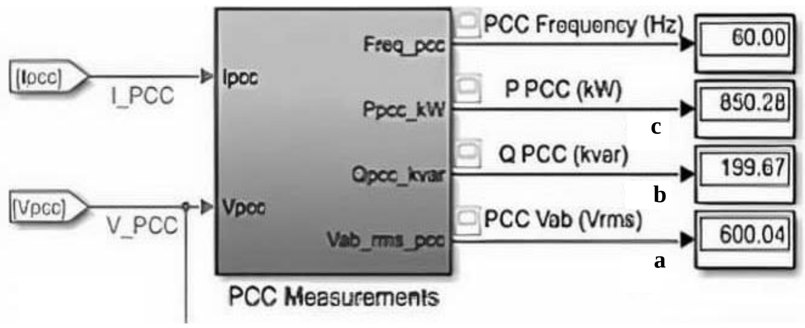

Figure 7. PCC measurement output of hybrid AC-DC microgrid with primary droop control (a) RMS voltage at PCC, (b) total reactive power in hybrid AC-DC microgrid, and (c) total active power in hybrid AC-DC microgrid

4. CONCLUSION

A well-known method for managing an autonomous grid is droop control. The primary method for distributing the demand power across the generators in autonomous microgrids without assistance from the electrical distribution grid is known as droop control. When a prime mover is operating a synchronous generator connected to an electrical grid, it is often utilized as the governor speed control mode.

The droop control component of this research deals with an alternating current/direct current hybrid microgrid. To precisely predict how each microgrid component would react under diverse conditions, many models for each component were developed. According to simulations, droop control may be used without the need for additional communication ports. Even though the frequency and voltage changes of the system are exceedingly minute, it is possible that adding additional secondary and tertiary hierarchical levels would increase the performance of the control logic. A more straightforward alternating current microgrid model with DC components or an interconnecting converter was developed to reduce fast and sub-transient dynamics that were not necessary to the study's aims.

REFERENCES

[1] K. Saadaoui, K. S. Rhazi, and A. Aboudou, "Hybridization and energy storage high efficiency and low cost," in *2020 6th IEEE Congress on Information Science and Technology (CiSt)*, Jun. 2020, pp. 33–41. doi: 10.1109/CiSt49399.2021.9357198.

[2] J. Liu, M. J. Hossain, J. Lu, F. H. M. Rafi, and H. Li, "A hybrid AC/DC microgrid control system based on a virtual synchronous generator for smooth transient performances," *Electric Power Systems Research*, vol. 162, pp. 169–182, Sep. 2018, doi: 10.1016/j.epsr.2018.05.014.

[3] N. Bhatt and S. Arora, "Droop control of inverter interfaced distributed generation," *Journal of Scientific Research and Reports*, pp. 1–6, Mar. 2022, doi: 10.9734/jsrr/2022/v28i230495.

[4] A. Khaledian and M. Aliakbar Golkar, "Analysis of droop control method in an autonomous microgrid," *Journal of Applied Research and Technology*, vol. 15, no. 4, pp. 371–377, Aug. 2017, doi: 10.1016/j.jart.2017.03.004.

[5] A. Rasoolzadeh and F. R. Salmasi, "Reduced-order dynamic model for droop-controlled inverter/converter-based low-voltage hybrid AC/DC microgrids – part 1: AC sub-microgrid," *IET Smart Grid*, vol. 1, no. 4, pp. 123–133, Dec. 2018, doi: 10.1049/iet-stg.2018.0069.

[6] C. Natesan, S. Ajithan, S. Mani, and P. Kandhasamy, "Applicability of droop regulation technique in microgrid - a survey," *Engineering Journal*, vol. 18, no. 3, pp. 23–36, Jul. 2014, doi: 10.4186/ej.2014.18.3.23.

[7] M. D. Ilić and S. Liu, "Structural modeling and control design using interaction variables," in *Hierarchical Power Systems Control*, 1996, pp. 61–81. doi: 10.1007/978-1-4471-3461-9_4.

[8] S. Augustine, J. E. Quiroz, M. J. Reno, and S. Brahma, "DC microgrid protection: Review and challenges," Albuquerque, NM, and Livermore, CA (United States), Aug. 2018. doi: 10.2172/1465634.

[9] M. Saeedifard, M. Graovac, R. F. Dias, and R. Iravani, "DC power systems: challenges and opportunities," in *IEEE PES General Meeting*, Jul. 2010, pp. 1–7. doi: 10.1109/PES.2010.5589736.

[10] H. Lotfi and A. Khodaei, "Hybrid AC/DC microgrid planning," *Energy*, vol. 118, pp. 37–46, Jan. 2017, doi: 10.1016/j.energy.2016.12.015.

[11] S. Gaurav and P. Agnihotri, "Enhanced droop control technique for parallel distributed generations in AC microgrid," in *Proceedings of Symposium on Power Electronic and Renewable Energy Systems Control*, 2021, pp. 429–438. doi: 10.1007/978-981-16-1978-6_37.

[12] R. Majumder, "Aspect of voltage stability and reactive power support in active distribution," *IET Generation, Transmission & Distribution*, vol. 8, no. 3, pp. 442–450, Mar. 2014, doi: 10.1049/iet-gtd.2013.0469.

[13] Y. Xia, W. Wei, M. Yu, X. Wang, and Y. Peng, "Power management for a hybrid AC/DC microgrid with multiple subgrids," *IEEE Transactions on Power Electronics*, vol. 33, no. 4, pp. 3520–3533, Apr. 2018, doi: 10.1109/TPEL.2017.2705133.

[14] H. Abdelgabir, "Dynamic modeling of nonlinear droop-controlled islanded microgrids and optimum placement of renewable energy sources," The University of Akron, Ohio, USA, 2018.

[15] K. Basiński, B. Ufnalski, and L. Grzesiak, "Hybrid MPPT algorithm for PV systems under partially shaded conditions using a stochastic evolutionary search and a deterministic hill climbing," *Power Electronics and Drives*, vol. 2, no. 37, pp. 49–59, 2017, doi: 10.5277/PED170212.

[16] N. Eghtedarpour and E. Farjah, "Power control and management in a hybrid AC/DC microgrid," *IEEE Transactions on Smart Grid*, vol. 5, no. 3, pp. 1494–1505, May 2014, doi: 10.1109/TSG.2013.2294275.

[17] R. Chakib, "Advanced control of a DFID-based wind turbine for its participation in system services: frequency adjustment, voltage adjustment and voltage sag withstand," (in French), Mohammed V University, EMI, Morocco, 2017.

[18] P. Kulkarni and S. P. Deshmukh, "Different converter topologies for solar photovoltaic system with methods for maximum power point tracking algorithms," *International Journal of Innovative Technology and Exploring Engineering*, vol. 8, no. 11, pp. 1112–1118, Sep. 2019, doi: 10.35940/ijitee.J1202.0981119.

[19] M. Eskandari, L. Li, M. H. Moradi, P. Siano, and F. Blaabjerg, "Simultaneous reactive power sharing and voltage regulation in an autonomous networked microgrid," *IET Generation, Transmission & Distribution*, vol. 14, no. 7, pp. 1366–1377, Apr. 2020, doi: 10.1049/iet-gtd.2019.0534.

[20] R. E. Carballo, F. Botteron, G. G. Oggier, and G. O. Garcia, "Dynamic model to design droop control strategies for parallel connected inverters," in *2017 XVII Workshop on Information Processing and Control (RPIC)*, Sep. 2017, pp. 1–6. doi: 10.23919/RPIC.2017.8214368.

[21] A. R. Årdal, T. Undeland, and K. Sharifabadi, "Voltage and frequency control in offshore wind turbines connected to isolated oil platform power systems," *Energy Procedia*, vol. 24, pp. 229–236, 2012, doi: 10.1016/j.egypro.2012.06.104.

[22] C. Kammer and A. Karimi, "Advanced droop control in islanded microgrids using dynamic phasor models," *IFAC-PapersOnLine*, vol. 50, no. 1, pp. 6642–6647, Jul. 2017, doi: 10.1016/j.ifacol.2017.08.1530.

[23] S. A. Díaz, A. de J. Chica, F. Sánchez, and C. A. Rodríguez, "Comparison of modeling methodologies for inverters in grid-connected mode, controlled by droop scheme," *International Journal of Applied Engineering Research*, vol. 13, no. 19, pp. 14241–14253, 2018.

[24] J. M. Rey, I. Jiménez-Vargas, P. P. Vergara, G. Osma-Pinto, and J. Solano, "Sizing of an autonomous microgrid considering droop control," *International Journal of Electrical Power & Energy Systems*, vol. 136, Mar. 2022, doi: 10.1016/j.ijepes.2021.107634.

[25] S. M. Muyeem, A. Al-Durra, and H. M. Hasanien, *Modeling and control aspects of wind power systems*. InTech, 2013. doi: 10.5772/3405.

[26] F. Dubuisson, "A new control strategy based on the droop concept for synchronization and power sharing in an autonomous microgrid in northern Canada," (in French), Quebec University, Montréal, Canada, 2019.

BIOGRAPHIES OF AUTHORS

Khalil Saadaoui was born in Morocco. He is a PhD student at the Laboratory of Networks, Computing Science, Telecommunication, and Multimedia (RITM), ESTC Casablanca, Hassan 2 University in Morocco. In 1997, he graduated with honors from Morocco's National School of Electricity and Mechanics with a degree in Electrical and Automation Engineering. His research activities include the hybrid energy, development of a control structure capable of optimizing cost with high efficiency. He is currently a teacher in several engineering schools and a consultant to international organizations. He can be contacted at khalil.saadaoui@ensem.ac.ma.

Kaoutar Senhaji Rhazi qualified professor in Electrical Engineering; at the School of Technology in Casablanca. Morocco. A graduate engineer in electrical engineering from the Mohammadia School of Engineers (EMI) in Rabat. Morocco (in 1991). Had the research preparation certificate (CPR) in telecommunications PhD in July 2006 (in electromagnetic compatibility). Passed academic qualification in the same field in 2014. Became higher education teacher in 2020. Current research interests are power electronics and electromagnetic compatibility. She can be contacted at senhaji.ksr@gmail.com.

Youssef Mejdoub was born in Morocco, in 1980. He received his PhD Thesis on Modeling of Multiconductor Transmission Lines, in 2014 from Cadi Ayyad University, Marrakech Morocco. Since 2016, he has been a Professor at the Superior school of technology (EST), University of Hassan II of Casablanca. He currently works at the Electrical Engineering Department, Superior school of technology. His current research interests are antennas, electromagnetic compatibility and MTL lines. He can be contacted at ymejdoub@yahoo.fr or youssef.mejdoub@univh2c.ma.

Abderraouf Aboudou received the M.Sc. degrees in electronic, electrotechnics and automatic in 1987, and the Ph.D. in physics in 1991, from Sciences and Technics University, Lille, France. He has been a professor of electrical engineering with Hassan II University, Casablanca, Morocco since 1991. He has authored or coauthored several refereed journal and conference papers. His actually research interests include the smart applications of renewable energy. He can be contacted at email: abderraoufaboudou@gmail.com.